ISSN: 2664-9640

Fault identification method of flexible DC distribution network based on Kullback-Leibler divergence

Dong Li, Hao Wu and Yuping Yang

University of Science and Engineering, Sichuan 643000, China

Abstract

Compared with the traditional AC distribution network, the flexible DC distribution network has higher power supply reliability and larger transmission capacity, but the fault identification method used for AC distribution network cannot be directly used in the fault identification of flexible DC distribution network. To this end, a Kullback-Leibler divergence-based fault identification method for flexible and straight distribution networks is studied. First, the trend of the positive and negative current signals at both ends of the line was analyzed under different faults. Then, KL dispersion is used to describe the degree of current correlation at both ends of the line under different faults. Finally, the faults are identified by threshold comparison. Simulation analysis and verification by PSCAD/EMTDC showed that the method is easy to implement, can correctly identify faults inside and outside the zone and select poles for faults inside the zone, and has high reliability.

Keywords

Flexible DC distribution networks, voltage sourced converters, Kullback-Leibler divergence, DC cables, Fault identification.

1. Introduction

The rapid development of power electronics has made DC systems once again a hot spot for power system research. Compared with the traditional AC power distribution system, the flexible DC power distribution system has a larger transmission capacity and higher power transmission efficiency; and the line loss is small, which has higher economy and power supply reliability. In addition, the flexible DC power distribution system facilitates the access of distributed energy sources[1-4]. However, when a fault occurs in the system, the fault current will rise rapidly in a very short period of time, and if the fault cannot be identified and isolated quickly, the whole system will be seriously damaged [5,6], so faster and more accurate fault identification is needed to reduce the damage caused by system faults to the system. This places higher demands on the rapidity and reliability of fault identification [7].

Literature [8] distinguishes between in-zone and out-zone faults by the ratio of the differential current Hausdorff distance inside and outside the zone. This method is easy to implement, but does not allow pole selection for in-zone faults. In the literature [9], the current gradient is first calculated by the current gradient algorithm and then compared with the rectified value to identify the in-zone and out-zone faults. This method is simple to implement, but only for the identification of bipolar faults. Literature [10] collects positive DC line currents at both ends of the line and solves the fault distance and transition resistance by the least squares method as a way to identify and locate faults. However, this method is only valid for bipolar faults. A new method of differential protection based on frequency band distribution is proposed in the literature [11]. The method extracts the high and low frequency energy of the differential current signal by discrete wavelet transform, and identifies the internal and external faults by

ISSN: 2664-9640

the high and low frequency energy ratio region. The above method is easy to implement, the feasibility is high, single only for a type of failure effective.

Based on this, a fault identification method based on current similarity that can be used for both single and double pole fault identification is investigated in this paper. The method characterizes the correlation degree of positive and negative current signals at both ends of the line through Pearson correlation coefficients, and uses the difference in Pearson correlation coefficients of positive and negative current signals at both ends of the line under different fault conditions for fault identification. Finally, the reliability and feasibility of the method are verified by simulation experiments.

2. Structure of flexible DC distribution network

The topology of the double-ended flexible DC distribution network is shown in Figure 1, the voltage level is 110 kV on the AC side and ±10 kV on the DC side, where: VSC1 and VSC2 are both fixed voltage control, the transformers connected to VSC on both AC sides are grounded, L1~L4 are DC cables of 4 km in length, including two lines of positive and negative poles, F1~F6 indicate fault points.

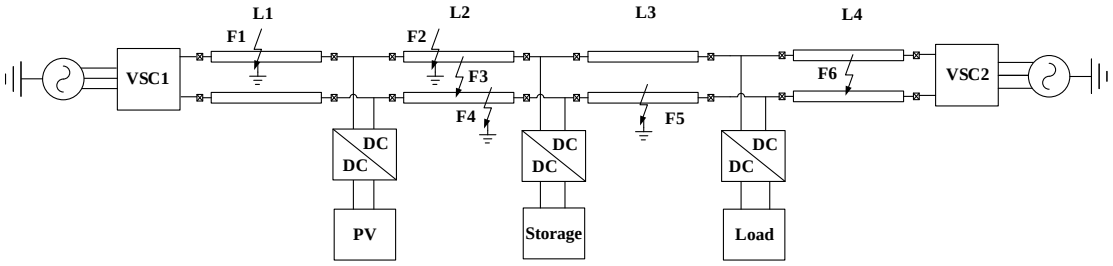

Figure 1: Topology of flexible DC distribution network

3. Current Characterization

After a DC-side fault occurs in the system, the current flowing through the line consists mainly of the rated current and the fault current component. The system after failure is analyzed by circuit superposition principle, and the system after failure can be regarded as the superposition network of the normal operating system and the system after failure. The current flow on the line can be expressed as:

$$I_{Fi} = I_{set} + \Delta I_f \tag{1}$$

Where I_{Fi} is the fault full current flowing through the line after the fault, I_{set} is the system rated current value, and ΔI_f is the fault current component. For later analysis, the positive direction of each section of the line current is specified as shown in Figure 2.

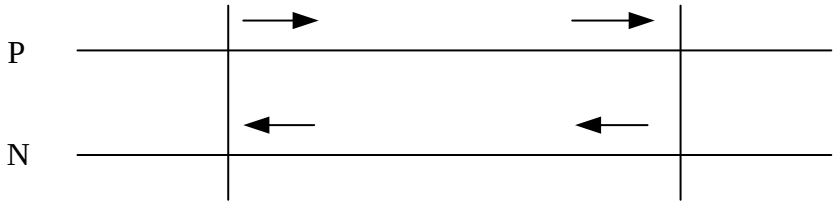

Figure 2: Positive direction of line current for each section of the system in normal operation

The positive and negative current waveforms at both ends of the line after different faults occur are shown in Figure 3.

ISSN: 2664-9640

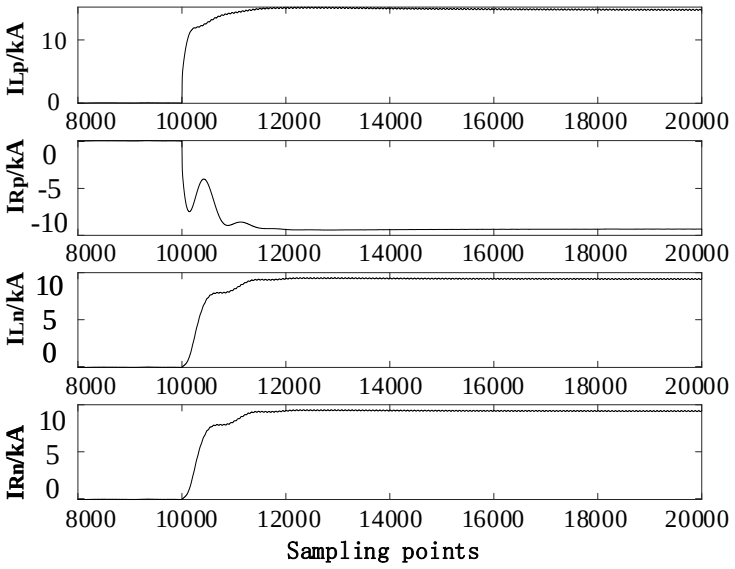

(a) Positive and negative current waveforms at both ends of the positive fault line in the zone

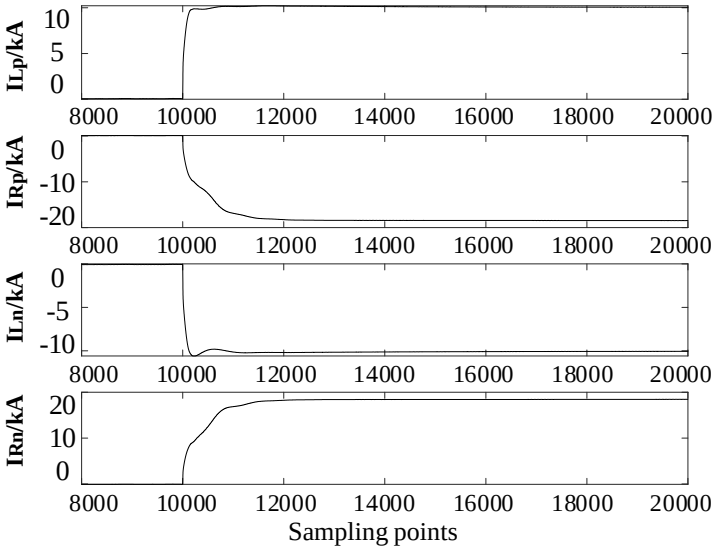

(b) Positive and negative current waveforms at both ends of the bipolar fault line in the zone

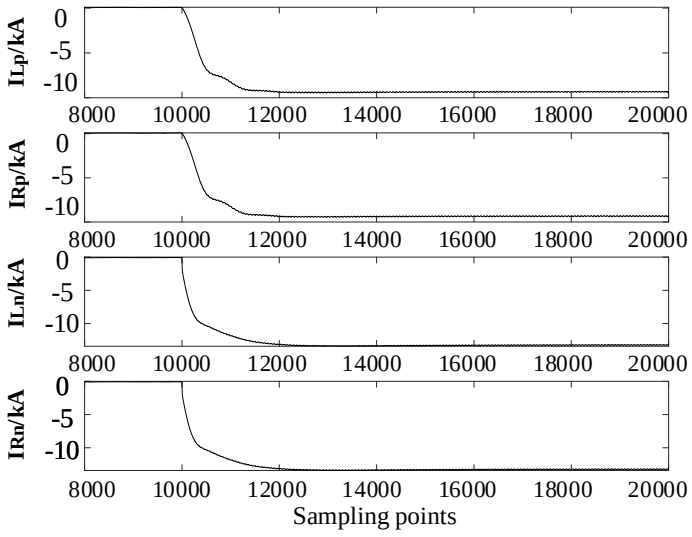

(c) Positive and negative current waveforms at both ends of the negative fault line outside the zone

ISSN: 2664-9640

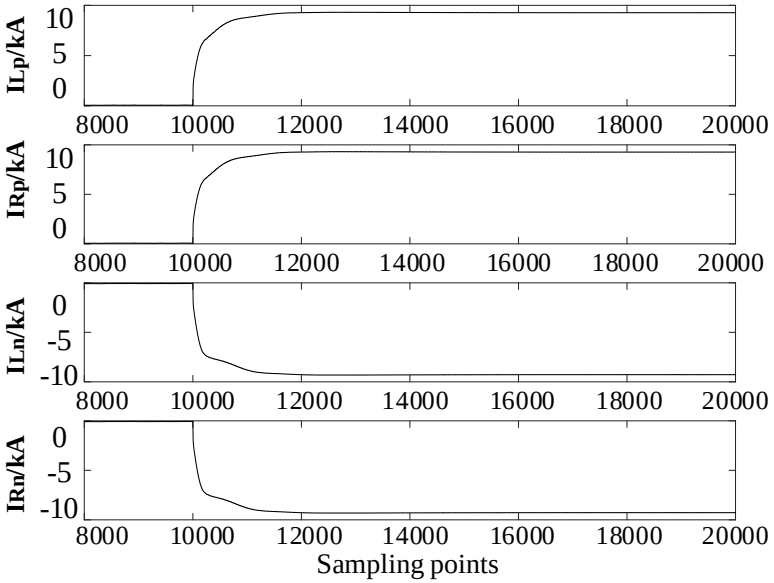

(d) Positive and negative current waveforms at both ends of the out-of-area bipolar fault line

Figure 3: Positive and negative current waveforms at both ends of the line after different faults

It is easy to see: the normal operation of the system (before the occurrence of the fault), the line ends of the positive and negative current signals to maintain a very high degree of similarity; when the system occurs outside the zone fault, the line ends of the positive and negative current signals will be affected by the fault current, but still maintain the same trend of change, the degree of similarity is still high; but when the system occurs within the zone fault, the line ends of the fault pole current signals will be under the influence of the fault current component the similarity will also decrease. As a result, fault identification can be performed from the perspective of the similarity of the current signals at both ends of the line.

4. Fault identification method based on Pearson correlation coefficient

Based on the analysis of the line current in the previous section, this paper starts from the similarity and uses the Kullback-Leibler divergence to express the similarity of the positive and negative current signals at both ends of the line. The Kullback-Leibler divergence of the current signals at both ends of the line is shown in equation (2).

$$KL(I_{xleft} \| I_{xright}) = \sum I_{xleft} \ln \frac{I_{xleft}}{I_{xright}} \tag{2}$$

Where I_{xleft} indicates the current signal at the left end of the positive (or negative) pole of the line; I_{xright} indicates the current signal at the right end of the positive (or negative) pole of the line; N is the number of current signal samples; $KL(I_{xleft} \| I_{xright})$ is the Kullback-Leibler divergence of the positive (or negative) pole of the line.

4.1. Identification of faults inside and outside the zone and fault pole selection

When the positive and negative current signals at both ends of the line meet $KL_i < KL_{set}$ (i=1, 2, 3 .....) three times in a row, it is determined that an intra-zone fault has occurred. KL_{set} is the fault determination threshold（after several simulation experiments, KL_{set} is taken as 1）. Thus, the in-zone and out-zone fault criteria are set as follows:

$$D_x = \begin{cases} 1 & Three\ consecutive\ samples\ meet\ KL_i < KL_{set} \\ 0 & Others \end{cases} \tag{3}$$

ISSN: 2664-9640

D_x is the fault discrimination function inside and outside the zone ($x = p$、n represents positive and negative poles respectively), when $D_x = 1$, it means that the fault occurs inside the zone, then the circuit breakers at both ends of the line act quickly to isolate the fault. When $D_p = 1$, represents the occurrence of positive ground fault in the zone; when $D_n = 1$, represents the occurrence of negative ground fault in the zone; when $D_p = D_n = 1$, represents the occurrence of double pole fault in the zone.

4.2. Identification Process

The flow chart of the fault identification method based on the improved Pearson correlation coefficient is shown in the following figure.

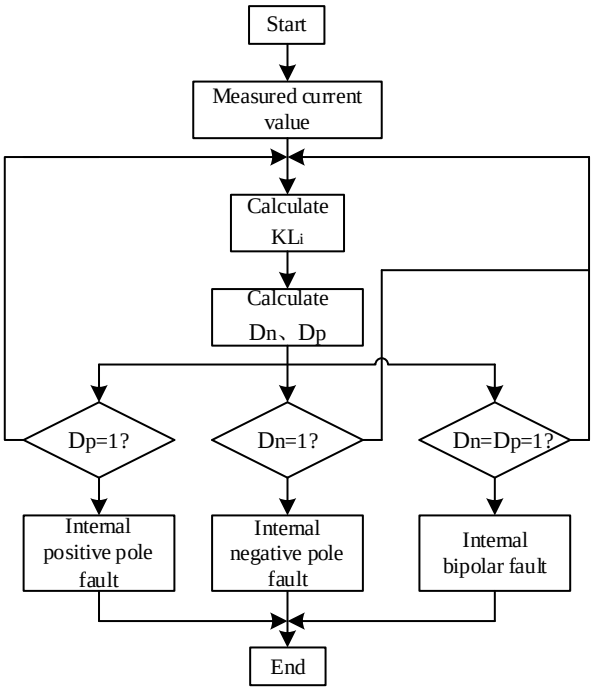

Figure 4: Fault identification flow chart

The in-zone and out-zone fault identification criterion and the in-zone fault pole selection criterion act simultaneously to confirm the occurrence of an in-zone fault and disconnect the DC circuit breakers at both ends of the fault line (configuration as shown in Figure 1), thereby isolating the fault.

5. Simulation Verification

In this paper, we build a double-ended flexible DC distribution network model in PSCAD/EMTDC as shown in Figure 1, and simulate faults from F1 to F6 respectively. F1 in L1, F5 in L3 and F6 in L4 are out-of-zone faults relative to L2; F2, F3 and F4 in L2 are in-zone faults, among which: F1 and F2 are positive ground faults; F4 and F5 are negative ground faults; F3 and F6 are bipolar faults, with a simulation sampling frequency of 10 kHz and a data window (i.e., the length of the data window for the calculation of equation (3) The requested data window length) is 1ms.

5.1. Testing of the ability to withstand transition resistance

In the DC distribution system, the maximum value of the transition resistance is about 20 Ω [12]. The line fault transition resistances are set to 5Ω, 10Ω, and 20Ω, and the results of each fault identification are shown in Table 1. Where KL_{p1}、KL_{p2} and KL_{p3} represent two

ISSN: 2664-9640

consecutive line ends positive current's Kullback-Leibler divergence; KL_{n1}、KL_{n2} and KL_{n3} represent two consecutive line ends negative current's Kullback-Leibler divergence.

Table 1: Identification results of various types of faults under different transition resistances

Name of fault	Transition resistances	KL_{p1}	KL_{n1}	KL_{p2}	KL_{n2}	KL_{p3}	KL_{n3}	D_p/D_n	Identification result
F1	5Ω	-0.028	0.001	-0.042	0.001	-0.042	-0.002	$D_p=0$ $D_n=0$	external faults
	10Ω	-0.008	0.000	-0.022	0.000	-0.023	-0.002	$D_p=0$ $D_n=0$	external faults
	20Ω	-0.017	-0.001	-0.024	0.000	-0.028	-0.001	$D_p=0$ $D_n=0$	external faults
F2	5Ω	0.023	-0.001	0.019	0.000	0.007	-0.001	$D_p=1$ $D_n=0$	Internal/positive
	10Ω	7.284	-0.011	7.333	-0.003	7.202	-0.001	$D_p=1$ $D_n=0$	Internal/positive
	20Ω	5.683	-0.008	5.607	-0.002	5.517	0.000	$D_p=1$ $D_n=0$	Internal/positive
F3	5Ω	5.275	-0.006	5.173	-0.001	5.124	0.000	$D_p=1$ $D_n=1$	Internal/bipolar
	10Ω	5.063	-0.005	4.944	0.000	4.911	0.000	$D_p=1$ $D_n=1$	Internal/bipolar
	20Ω	7.701	8.057	7.803	8.172	7.596	7.978	$D_p=1$ $D_n=1$	Internal/bipolar
F4	5Ω	5.958	6.340	5.909	6.304	5.705	6.115	$D_p=0$ $D_n=1$	Internal/negative
	10Ω	5.173	5.576	5.071	5.486	4.902	5.331	$D_p=0$ $D_n=1$	Internal/negative
	20Ω	4.762	5.197	4.637	5.084	4.499	4.960	$D_p=0$ $D_n=1$	Internal/negative
F5	5Ω	-0.010	6.900	-0.003	6.955	-0.001	6.861	$D_p=0$ $D_n=0$	external faults
	10Ω	-0.007	5.688	-0.002	5.639	0.000	5.582	$D_p=0$ $D_n=0$	external faults
	20Ω	-0.005	4.797	-0.001	4.729	0.000	4.710	$D_p=0$ $D_n=0$	external faults
F6	5Ω	-0.004	5.592	0.000	5.515	0.000	5.517	$D_p=0$ $D_n=0$	external faults
	10Ω	0.003	0.087	0.006	0.075	0.000	0.059	$D_p=0$ $D_n=0$	external faults
	20Ω	0.002	0.028	0.005	0.017	-0.001	0.013	$D_p=0$ $D_n=0$	external faults

As can be seen from Table 1, the proposed algorithm is still able to correctly identify faults in the case of 20 Ω transition resistance.

5.2. Testing of fault distance adaptability

For the double-ended direct flexible flow distribution network topology shown in Figure 1, the identification results of various types of faults occurring at different locations (1km, 2km and 3km from the left end of the line) from the left end of each line are shown in Table 2.

Table 2: Identification results of various types of faults at different fault distances

Name of fault	Fault distance	KL_{p1}	KL_{n1}	KL_{p2}	KL_{n2}	KL_{p3}	KL_{n3}	D_p/D_n	Identification result
F1	1km	0.003	0.010	-0.007	0.003	0.019	0.000	$D_p=0$ $D_n=0$	external faults
	2km	-0.083	0.006	-0.081	0.003	-0.081	-0.001	$D_p=0$	external faults

ISSN: 2664-9640

								D_n=0	
	3km	-0.016	0.010	-0.018	0.007	-0.019	-0.001	D_p=0 D_n=0	external faults
F2	1km	29.686	0.002	32.059	0.011	33.428	0.007	D_p=1 D_n=0	Internal/positive
	2km	16.471	-0.017	17.702	-0.006	18.274	0.000	D_p=1 D_n=0	Internal/positive
	3km	6.230	-0.009	6.735	0.003	7.065	0.009	D_p=1 D_n=0	Internal/positive
F3	1km	25.439	25.442	27.290	27.317	28.263	28.317	D_p=1 D_n=1	Internal/bipolar
	2km	13.267	13.603	14.092	14.440	14.331	14.692	D_p=1 D_n=1	Internal/bipolar
	3km	4.099	4.427	4.241	4.579	4.224	4.574	D_p=1 D_n=1	Internal/bipolar
F4	1km	0.001	25.596	0.008	27.598	0.006	28.760	D_p=0 D_n=1	Internal/negative
	2km	-0.014	14.520	-0.005	15.571	-0.001	16.071	D_p=0 D_n=1	Internal/negative
	3km	-0.008	5.712	0.001	6.145	0.007	6.433	D_p=0 D_n=1	Internal/negative
F5	1km	0.001	-0.533	0.008	-0.312	0.002	-0.115	D_p=0 D_n=0	external faults
	2km	0.007	0.403	0.009	0.396	0.004	0.359	D_p=0 D_n=0	external faults
	3km	0.008	0.281	0.012	0.245	0.004	0.005	D_p=0 D_n=0	external faults
F6	1km	0.338	0.337	-0.094	-0.094	-0.095	-0.095	D_p=0 D_n=0	external faults
	2km	0.391	0.388	-0.001	-0.001	0.034	0.034	D_p=0 D_n=0	external faults
	3km	0.162	0.161	-0.194	-0.194	-0.003	-0.002	D_p=0 D_n=0	external faults

As can be seen from Table 2, the fault identification algorithm has high fault distance adaptability.

5.3. Testing of noise interference resistance

Noise disturbances may have an impact on the reliability of the recognition algorithm. In subsection 4.1, the influence of partial noise has been considered by adding reliability coefficients to rectify the calculation results. Table 3 shows the identification results of various types of faults after adding the signal-to-noise ratio of 30 dB, 40 dB and 50 dB noise signals, respectively.

Table 3: Identification results of various types of faults under the influence of different signal-to-noise ratio noise

Name of fault	Signal-to-noise ratio	KL_{p1}	KL_{n1}	KL_{p2}	KL_{n2}	KL_{p3}	KL_{n3}	D_p/D_n	Identification result
F1	20dB	-0.689	0.443	-0.357	0.414	-0.431	-0.021	D_p=0 D_n=0	external faults
	30dB	0.031	-0.003	-0.050	-0.038	-0.175	-0.009	D_p=0 D_n=0	external faults
	40dB	-0.062	-0.027	-0.071	0.010	-0.079	0.000	D_p=0 D_n=0	external faults
F2	20dB	16.265	-0.042	17.875	0.024	18.878	-0.087	D_p=1 D_n=0	Internal/positive

ISSN: 2664-9640

	30dB	16.553	-0.203	17.840	-0.145	18.314	-0.105	D_p=1 D_n=0	Internal/positive
	40dB	16.395	-0.026	17.610	-0.010	18.256	-0.002	D_p=1 D_n=0	Internal/positive
F3	20dB	14.425	13.669	14.885	14.436	15.181	14.643	D_p=1 D_n=1	Internal/bipolar
	30dB	13.617	13.018	14.263	14.025	14.479	14.158	D_p=1 D_n=1	Internal/bipolar
	40dB	13.398	13.624	14.232	14.448	14.452	14.658	D_p=1 D_n=1	Internal/bipolar
F4	20dB	0.215	15.292	-0.725	16.296	-0.537	16.133	D_p=0 D_n=1	Internal/negative
	30dB	0.491	14.652	0.486	15.473	0.430	16.023	D_p=0 D_n=1	Internal/negative
	40dB	-0.047	14.488	-0.042	15.528	-0.023	16.042	D_p=0 D_n=1	Internal/negative
F5	20dB	-0.284	0.508	-0.103	0.316	-0.100	0.424	D_p=0 D_n=0	external faults
	30dB	0.076	0.296	0.102	0.238	0.131	0.163	D_p=0 D_n=0	external faults
	40dB	0.210	0.335	0.180	0.332	0.176	0.293	D_p=0 D_n=0	external faults
F6	20dB	0.793	0.411	0.097	-0.542	0.305	-0.434	D_p=0 D_n=0	external faults
	30dB	0.344	0.517	0.011	0.086	0.114	0.090	D_p=0 D_n=0	external faults
	40dB	0.306	0.507	-0.089	0.079	-0.061	0.110	D_p=0 D_n=0	external faults

As can be seen from Table 3, the proposed algorithm can still recognize faults inside and outside the zone under the influence of 20dB white noise and select poles for faults in the zone. However, when 10dB white noise is added, some faults will fail to be identified, so the proposed algorithm can tolerate the effect of 20dB white noise.

6. Conclusion

In this paper, a fault identification method based on Pearson correlation coefficient of DC side fault current is proposed for VSC double-end flexible DC distribution network. The method can realize the fault identification of the whole line; it can accurately identify the faults inside and outside the zone and select the poles for the faults inside the zone under the consideration of different transition resistances, different fault distances and different signal to noise ratios; the identification criterion is simple to calculate and does not require high sampling accuracy; the method does not need to start the criterion and meets the requirement of quick-activity.

The shortcoming of this method is that it does not consider the possible data loss during the transmission of the sample numbers, and further research will be conducted to address this shortcoming in the subsequent study.

Acknowledgements

This work is supported by National Nature Science Foundation of The Project of Sichuan provincial science and Technology Department (Grant No. 2020YFG0178, 2021YFG0313); The artificial intelligence key laboratory of Sichuan province Foundation (2019RYY01)

ISSN: 2664-9640

References

[1] D.Q. Bi, F. Zhang, X.J. Zeng, et al. Fault recovery study of ship DC regional distribution network. Power System Protection and Control, Vol. 43(2015) No.19, p. 60-65.

[2] NOROOZIANA R, ABEDIB M, GHAREHPETIANB G B, et al. Distributed resources and DC distribution system combination for high power quality. Electrical Power and Energy Systems, Vol. 32(2010) No.7, p. 769-781.

[3] D.Z. Jiang, H. Zheng. Current status and outlook of DC distribution network research. Power System Automation, Vol. 36(2012) No. 8, p. 98-104.

[4] D. Wang, Y.R. Liu, X. Liang, et al. Study on voltage level sequence of DC distribution network. Power System Automation, Vol. 39(2015) No. 9, p. 19-25.

[5] B. Li, J.W. He. Fault analysis and current limiting method for flexible DC distribution system, Chinese Journal of Electrical Engineering, Vol. 35(2015) No.12, p. 3026-3036.

[6] MEHDI M, ZAMANI M A, JOSE I C, et al. Protection of AC and DC distribution systems Embedding distributed energy resources: A comparative review and analysis, Renewable and Sustainable Energy Reviews, Vol. 51(2015) No.1, p. 1159-1578.

[7] J.W. He, B.Li, Y. Li, et al. Fast directional longitudinal protection scheme for multi-terminal flexible DC networks, Chinese Journal of Electrical Engineering, Vol. 37(2017) No.23, p. 6878-6887.

[8] M.Huang. *Research on relay protection scheme for ring DC distribution network* (Ph.MS., North China Electric Power University, China 2019.)

[9] Y. Zeng. *Research on fault routing and protection method for radial DC distribution network* (Ph.MS, Shandong University, China 2019.)

[10] P.Gao, W.T. Huang, N.L. Tai, Z.J. Ma, Y. Wang, C.B. Li. Transient current based MMC-LVDC bipolar short circuit fault location method , Power System Automation, Vol. 44(2020) No.17, p. 127-135.

[11] M. Li. *Research on protection of flexible DC distribution network* (Ph.D. Beijing:North China Electric Power University, China 2018.)

[12] B. LI, J.W. HE, Y. LI, et al. Single-ended protection scheme based on boundary characteristic for the multiterminal VSC-based DC distribution system. Proceedings of the CSEE, Vol. 36(2016) No. 21, p. 5741-5749.